*Journal of Thermal Analysis Vol. 46 (1996) 1081-1092*

Dedicated to Professor Bernhard Wunderlich on the occasion of his 65th birthday

# THERMAL PROPERTIES OF A MOLECULE IN A CONSTRAINED STATE
## Dye-amylose inclusion complex

*Suk-Fai Lau, A. J. Sosnowik, Ling-Siu Choi*, J. H. Callahan* and Oh-Kil Kim**

Research Center, Hercules Incorporated, Wilmington, DE 19808–1599
*Chemistry Division, Naval Research Laboratory, Washington, DC 20375-4325, USA

## Abstract

The thermal properties of a dye molecule (guest) inside the cavity of a host amylose helix were studied by TGA, DSC, and Thermal Desorption MS. The results show that the degradation temperature of dye shifts to a higher temperature by approximately 20°C.

**Keywords:** chemical ionization MS, constrained dye, DSC, dye-amylose inclusion complex, Tandem MS, TGA, Thermal Desorption MS

## Introduction

Supramolecular chemistry is one of the most interesting recent topics [1]. Inclusion systems belong to a supramolecular domain and attract a great deal of attention for their role in molecular recognition. Particularly with cyclodextrins as hosts, numerous studies have been done on binding characteristics, stability of the inclusion complex, and applications [2–6]. Some studies recently explored a unique inclusion system with long chain guest molecules such as poly(ethylene glycol) or poly(propylene glycol) which is included by a stack of cyclodextrin units, forming a necklace-like rotaxane [7]. Similar to cyclodextrin but more flexible in size (number of glucose units per turn) [8–10] and length of the guest-binding sites, amylose has also been known to form inclusion complexes with various organic compounds [11–17] through hydrophobic interactions. Amylose is a linear natural polymer which is composed of *D*-glucose linked through an α-1,4-glucosidic bond. Many complexation studies have been done with cyclodextrin and amylose. However, little is known about the thermal properties of solid inclusion complexes, particularly that of the constrained guest in the inclusion.

In this paper, we report the studies of thermal properties of constrained dye molecules in amylose inclusion complexes by thermal analysis and mass spec-

*0368–4466/96/ $ 5.00*

*John Wiley & Sons, Limited*
*Chichester*

trometry. With an aim to develop thermally stable nonlinear optical materials, we are concerned with the molecular influence of the constrained state on its thermal properties, especially as to whether or not the constrained state can contribute a significant improvement to the thermal stability of guest molecules in the inclusion state.

For this study, we chose amylose as a host because amylose can assume a helical rigid rod structure which is capable of including long-chain hydrophobic guest molecules and optical-quality films can be obtained from the aqueous solution of inclusion complexes. 4[4(dimethylamino) styryl]-1-docosyl-pyridinium bromide (hemicyanine dye) was selected as the guest because its molecules are strongly hydrophobic and shows a second-order optical nonlinearity.

## Experimental

Amylose and 4[4(dimethylamino) styryl]-1-docosylpyridinium bromide were bought from Aldrich Chemical Company. The dye was purified by crystallization from ethanol.

### *Thermal analysis*

1. Thermal Gravimetric Analysis (TGA)

TGA curves were generated using a TA Instruments 2100 Thermal Analysis System equipped with a 2950 robotic TGA module. Samples were placed in an open platinum pan, under a nitrogen purge and heated at 1°C $min^{-1}$ from room temperature to 400°C.

2. Differential Scanning Calorimetry (DSC)

DSC curves were obtained using a TA Instruments 2200 Thermal Analysis System equipped with a 2910 modulated DSC. Samples of approximately 1 milligram weight were enclosed in a crimped aluminum pan, placed in the cell under a nitrogen purge, and scanned from 125°C to degradation at 1°C $min^{-1}$ while modulating the temperature 1.5°C every 80 seconds. First heat data were reported as heat flow *vs.* temperature.

### *Mass spectrometry*

1. Thermal Desorption Mass Spectrometry (TDMS)

Thermal desorption mass spectrometry was performed on a Finnigan TSQ-70 triple quadrupole mass spectrometer equipped with a direct exposure probe (DEP). It consisted of a 12 mm diameter stainless steel shaft and a removable platinum wire loop probe tip. Samples were applied as liquids to the platinum

wire loop tip and allowed to evaporate to dryness. The DEP was then introduced into the instrument and positioned in the ion source. A preprogrammed current ramp was then applied to the platinum wire, increasing the probe temperature at a controlled rate. For these experiments, the probe current was held at approximately 50 milliamps (mA) for 6 seconds and then increased to 900 mA at a rate of 550 mA $min^{-1}$. With 70 eV electrons, the sample was thermally desorbed from the DEP into the ion source. The instrument was scanned from mass-to-charge ratio (*m/z*) 50 to *m/z* 600 at a rate of 1 scan per second.

Due to the nature of the probe, it is not possible to accurately measure the probe temperature, consequently only applied current values are specified here. Probe behavior is consistent from one sample to the next and comparisons of desorption behavior from different samples are valid.

2. Chemical ionization (CI) mass spectrometry

Chemical ionization mass spectrometry was performed using ammonia as a reagent gas at a pressure of 5 torr. Samples were desorbed directly from the thermal desorption probe into a reagent bath gas that consisted primarily of $[NH_4]^+$and $[NH_3 + NH_4]^+$ formed by bombardment of ammonia with 70 eV electrons.

3. Tandem mass spectrometry

Tandem mass spectrometry was performed using 0.5 millitorr of argon in the collision cell (second quadrupole). Ions were mass-selected using the first quadrupole, which was tuned to pass only a single mass-to-charge. Ions then underwent collisions with argon in the second quadrupole at energies of 25 eV, and the fragments were mass analyzed by the third quadrupole.

## *Sample preparation*

### Formation of inclusion complex

The dye, 0.106 g, was dissolved in 100 ml DMSO at 80 °C. Amylose, 1.5 g, was then added to the DMSO solution. The solution of dye and amylose was added to 1 liter of water. The resulting solution was dialyzed against water for two weeks with water changed twice a day. The dialyzed solution was filtered and freeze-dried, leading to red solid [18]. From the elemental analysis, the supramolecule is a one to one ratio of host: guest. The amount of dye is about 13% by weight of the supramolecule.

### Sample preparation for MS

For studies of the dye alone, 3 mg of the dye was dissolved in one ml of methanol. A microliter pipet was used to deposit 1 μl of the solution (3 μg of

material) on the probe and the solvent was evaporated. The sample was then thermally desorbed with the aforementioned temperature ramp.

For studies of the inclusion complex, 1 μl of an aqueous solution (10 mg $ml^{-1}$) of the inclusion complex was applied to the probe tip and the water evaporated. The sample was analyzed as described above.

A mixture of dye and amylose in DMSO was also studied to evaluate a mixture where both would be present, but not in the form of an inclusion complex.

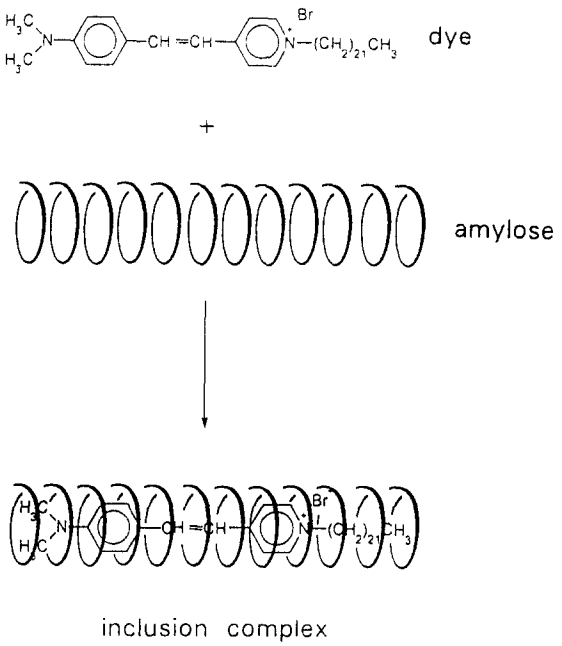


## Results and discussion

The first derivatives of weight loss with respect to temperature are obtained for TGA studies. The peak pattern and position offer thermal information on the inclusion dye. Figure 1 exhibits the TGA results for the samples: dye, amylose, amylose-dye inclusion complex, and amylose and dye mixture. For dye alone, we observe one major degradation peak at 267 °C with a shoulder at 253 °C. For amylose alone, we observe a single broad degradation peak with a maximum at 288 °C. When equal moles of amylose and dye are mixed, TGA results show only one broad degradation peak at 288 °C, the same temperature as the amylose itself, but with greater intensity. Since there are equal molar ratios of amylose and dye, and the molecular weight of amylose is larger than dye (4 100 *vs.* 613.8, respectively), the amylose is the dominating contributor to the shape of the degradation curve and the difference in intensity between the amylose alone and the amylose-dye mixture, is due to the presence of the dye.

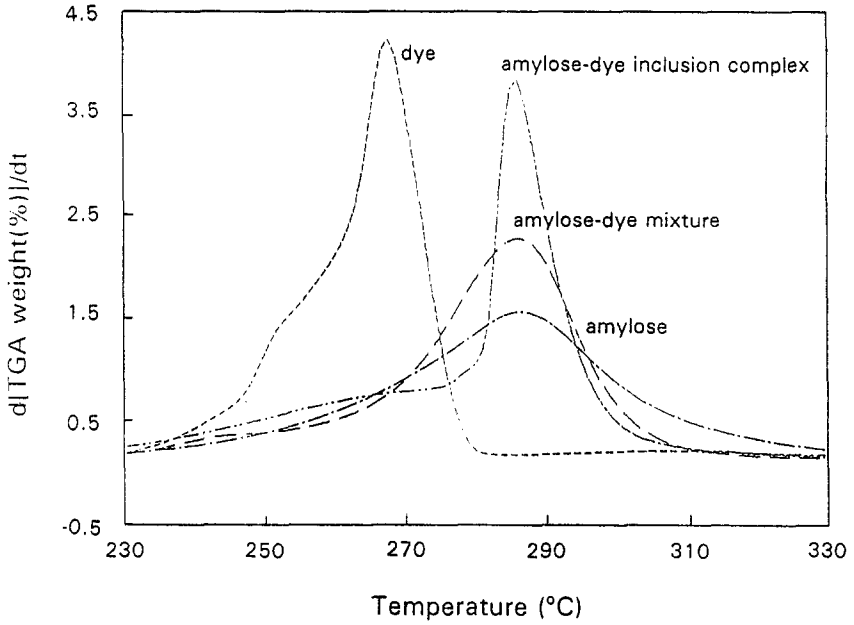


**Fig. 1** TGA curves of dye, amylose, inclusion complex, and amylose-dye mixture

For the amylose-dye inclusion complex, there is one major peak at 288°C and a shoulder at approximately 270°C. Comparing the composite curves of the dye alone, the amylose alone and the amylose-dye inclusion complex, we can draw the following conclusions: the shoulder of the curve at 270°C corresponds to the degradation shoulder of the free dye at 253°C, and the inclusion complex main peak at 288°C represents the degradation of the amylose and the immediate degradation of the enclosed dye once the protective coating of the amylose is gone. This implies that enclosing dye inside the amylose delays both the shoulder and the main degradation peaks of the dye by approximately 20°C. For β-cyclodextrin and vitamin D, the effect of inclusion in protecting guest molecules against thermal degradation has been reported [19]. When vitamin D is heat-treated at 80°C either as a free form or as a mechanical mixture, no vitamin D could be detected after 24 hours. When vitamin D-(β-cyclodextrin) complex is subjected to the same condition, 41% of the original vitamin content remains even after 43 days.

From the DSC curve of the dye alone we observe two endothermic transitions (Fig. 2). A minor endotherm, appears at 229°C, is believed to be the rearrangement of dye solid to a highly ordered crystalline structure; and a major sharp endotherm, at 253°C, is the melting of the crystalline dye. The DSC curve of amylose alone shows a broad minor endotherm at approximately 253°C that goes immediately into an exothermic decomposition. When the dye-amylose inclusion complex was run under the same conditions, no sharp endothermic peak was observed in the temperature region where the dye alone

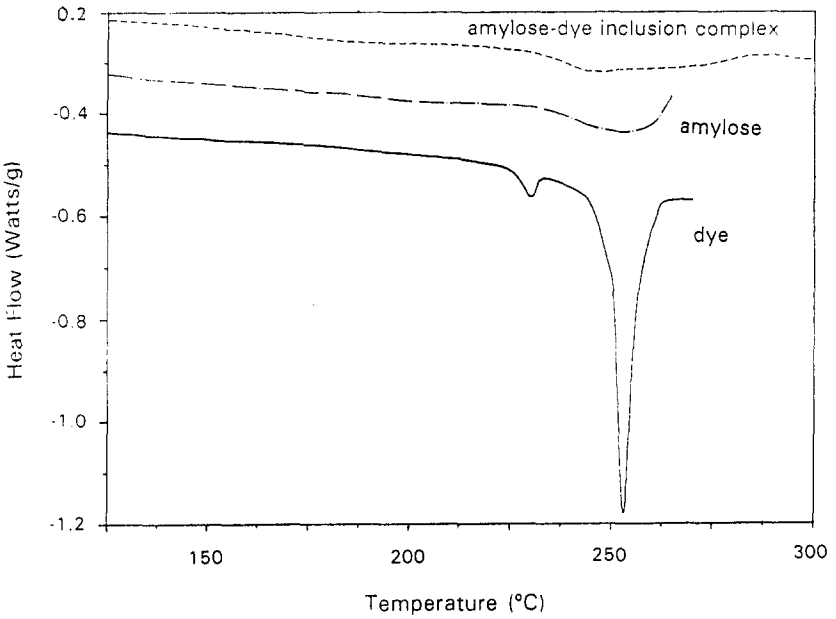


**Fig. 2** DSC curves of dye, amylose, and inclusion complex

melted, and no exotherm was observed that would correspond to the degradation of the amylose alone. One explanation for not observing an endothermic melting of the dye is due to the fact that only a single dye molecule can be enclosed inside the amylose helix cavity. Since a single molecule cannot form a crystalline structure, no endothermic melting should be observed.

The thermal effect on the confined dye can also be studied by thermal desorption mass spectrometry (TDMS). Figure 3(a) shows the mass spectrum obtained from the thermal desorption of the dye alone. The ion at *m/z* 224 most likely arises from the cleavage of the docosyl group from the pyridine ring, while the ions at *m/z* 57, and 43 are characteristic alkyl fragments from the docosyl chain. Desorption profiles for *m/z* 224, the sum of *m/z* 43 and *m/z* 57, and the total reconstructed ion current are plotted in Fig. 3b. The desorption profiles in Fig. 3b show that peak ion currents are observed at scan 67, which corresponds to a probe current of 600 mA. Figure 4a and 4b show a representative mass spectrum and desorption profiles for the inclusion complex. The plotted ion abundances are the same as those in Fig. 3b. These profiles show that the peak ion currents have shifted for this sample, reaching a maximum at approximately scan 87 (740 mA). These results suggest that the desorption and decomposition of the dye are shifted to a higher temperature in the inclusion complex, consistent with the TGA results.

It can also be argued that the ions attributed to thermal decomposition arise from the normal fragmentation pattern observed in electron ionization mass

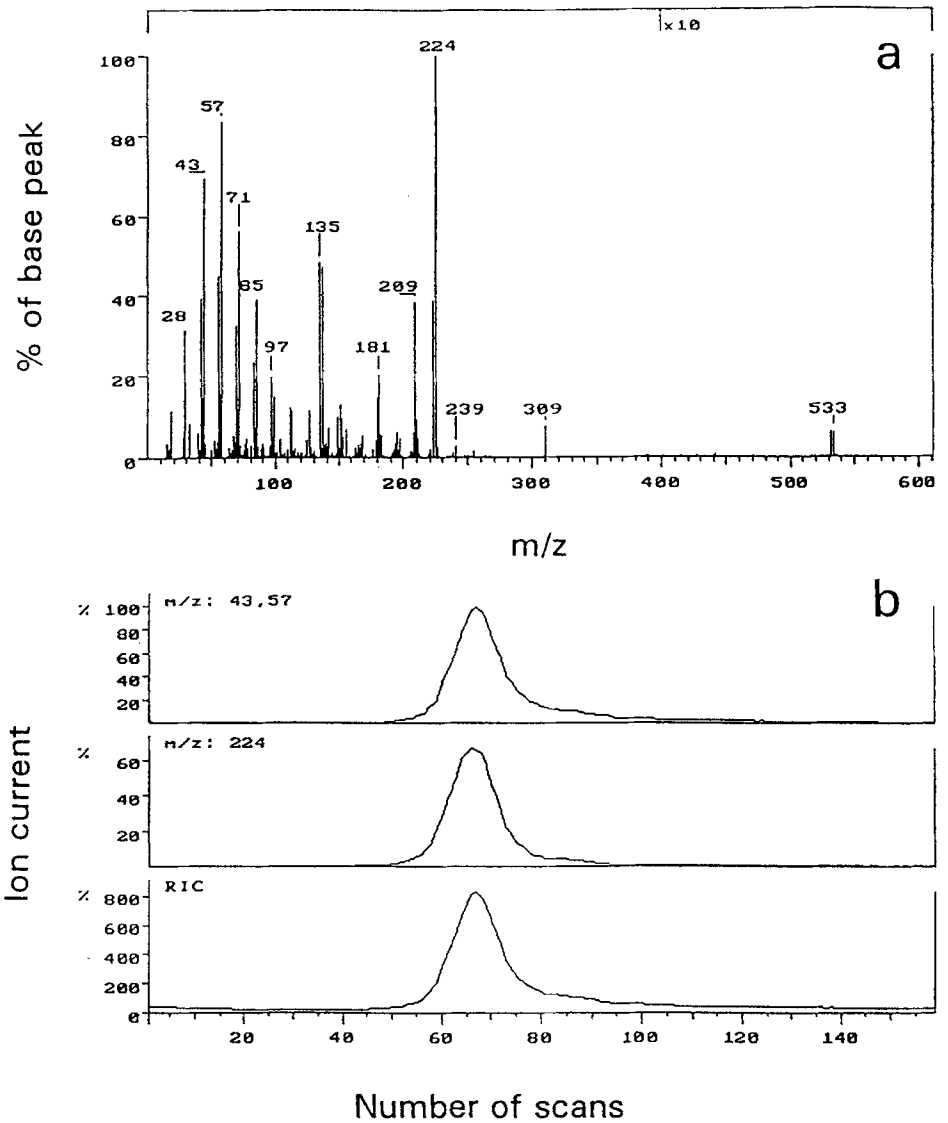


**Fig. 3** (a) Mass spectrum of dye; (b) ion current *vs.* number of scans for the ion fragments of dye

spectrometry. Such a possibility is supported by the observation of the desorption of intact molecular ions (*m/z* 533), suggesting that electron-induced fragmentation of the intact molecule could account for the observed fragments. Thus, there is some ambiguity in these results. However, the interference caused by electron-induced fragmentation can be eliminated by using a soft ionization technique, such as ammonia chemical ionization, wherein little frag-

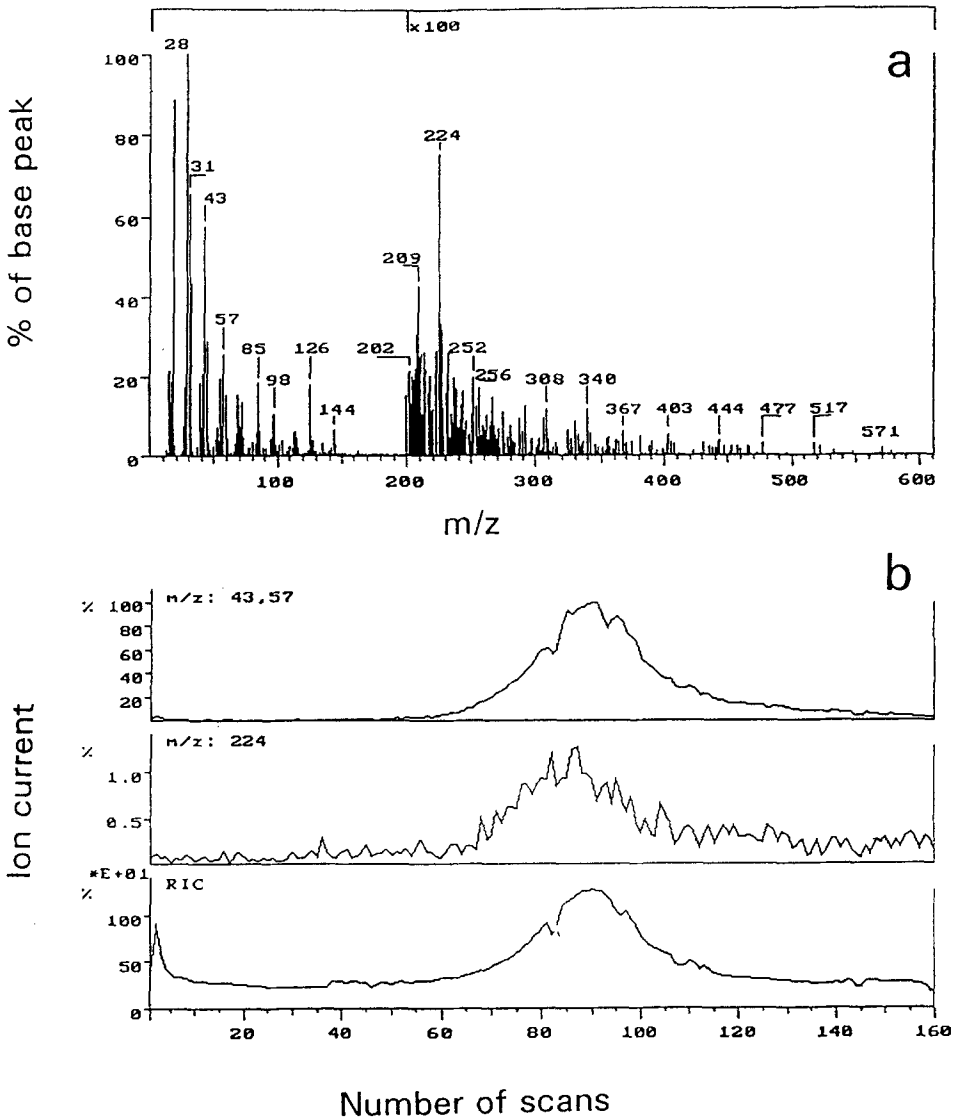


**Fig. 4** (a) Mass spectrum of inclusion complex; (b) ion current *vs.* number of scans for the ion fragments of inclusion complex

mentation of molecular ions is observed. For example, when the dye alone was thermally desorbed into 5 torr of ammonia, the principal ion observed in the spectrum appears at *m/z* 225 (Fig. 5a). This corresponds to the protonated ion that results from the cleavage of the docosyl group from the pyridine ring. Under the conditions employed in chemical ionization mass spectrometry, it is unlikely that the species at *m/z* 225 arises from either fragmentation of the dye

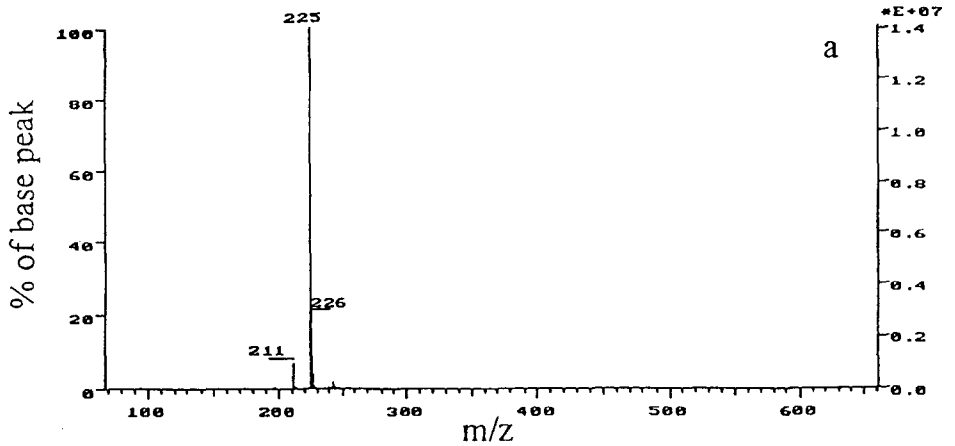


**Fig. 5a** Thermal desorption chemical ionization mass spectra of dye deposited from methanol solution

(in the gas phase) followed by protonation of the fragment, or protonation of the intact dye in the gas phase, followed by fragmentation. The more likely explanation is that the dye undergoes thermal decomposition on the surface, followed by desorption of the products and their protonation in the gas phase. Consequently, ammonia chemical ionization mass spectrometry is probably a more accurate way to characterize the thermal decomposition of the dye. Given that this is the case, thermal desorption mass spectra were obtained for the dye alone, a DMSO solution of the dye and amylose (non-inclusion complex) and an aqueous solution of the dye-amylose inclusion complex. The formation of the protonated thermal decomposition product at *m/z* 225 was used to compare the three cases. Initial studies unfortunately indicated that background interferants are formed at *m/z* 225 when amylose is present, complicating the experiment (Fig. 5b). The application of tandem mass spectrometry alleviated the problems of interferences at *m/z* 225. In the tandem mass spectrometry experiment, the ion at *m/z* 225 is selected by the first quadrupole, collided at a specified collision energy with a target gas (Ar in this case) and the fragments from this process are monitored with the third quadrupole. Studies of the dye alone (without amylose) show that the ion at *m/z* 225 undergoes characteristic fragmentation with the neutral loss of methane or methyl radicals (to form ions at *m/z* 209 and 210), the neutral loss of dimethylamine and dimethylamine radical (to give *m/z* 180 and 181) and the loss of dimethylaminobenzene (to give *m/z* 104) (Fig. 5c). These five ions were thus used to monitor the formation of the protonated decomposition product at *m/z* 225. Thus, even in the presence of the complex amylose matrix, the thermal decomposition product at *m/z* 225 could be monitored, while rejecting other background at *m/z* 225. The desorp-

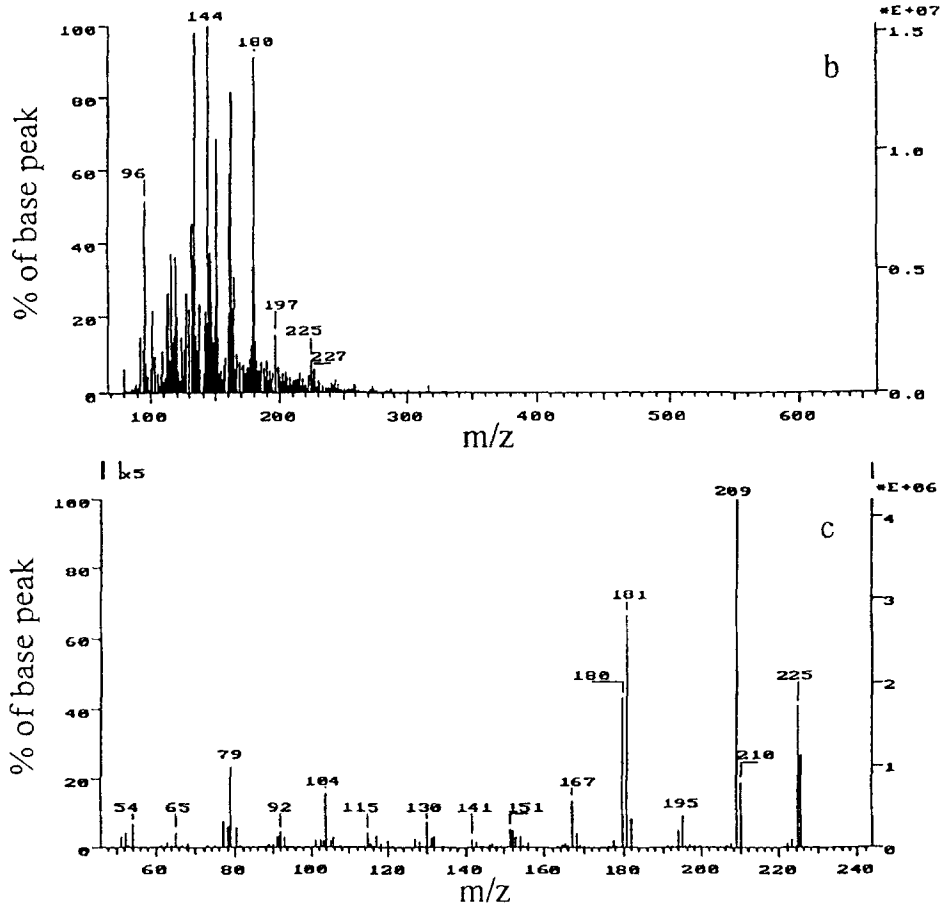


**Fig 5b,c** Thermal desorption chemical ionization mass spectra of (b) the aqueous dye-amylose complex (note the relatively high background level around *m/z* 225); and (c) the tandem mass spectrum of *m/z* 225 (collision energy 25 eV, 0.5 millitorr of Ar) formed by the thermal desorption of dye into ammonia under chemical ionization conditions

tion profiles for each of the solutions are shown in Fig. 6a–c. The ion currents for *m/z* 225 and for the sum of *m/z* 104, 180, 181, 209 and 210 are plotted. The results show that, with the same desorption temperature ramp, the maximum formation of the decomposition product occurs at scan 68 for the DMSO solution of dye-amylose (non-inclusion complex), at scan 68 for dye alone (from methanol solution) and at scan 86 for the aqueous dye-amylose complex. The latter case clearly indicates that the thermal decomposition product is formed at a higher temperature for the inclusion complex, and is consistent with observations noted above in the thermal desorption experiments.

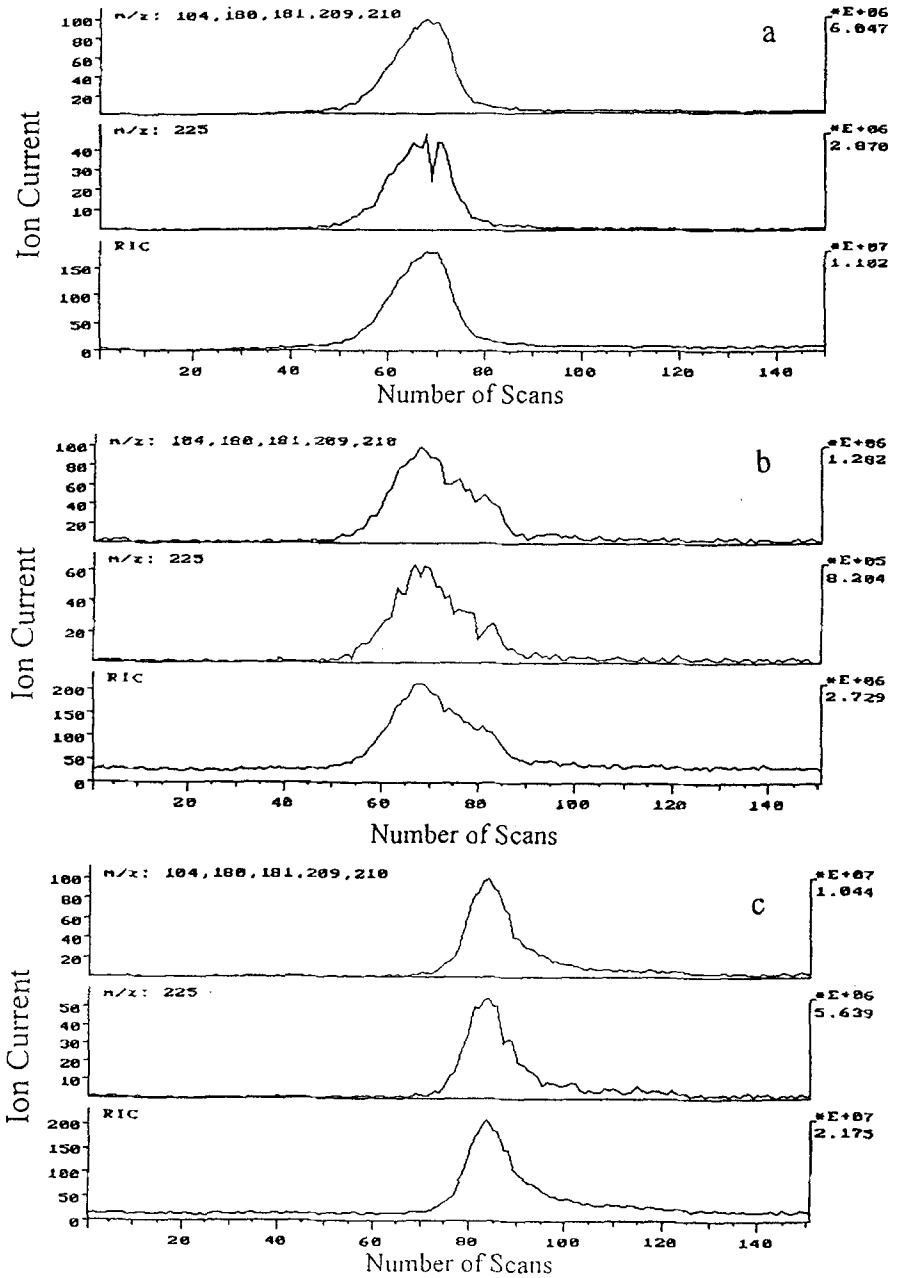


**Fig. 6** Thermal desorption chemical ionization tandem mass spectrometry ion current profiles for the total ion current, *m/z* 225 (mass-selected ion) and fragment ions (sum of *m/z* 104, 180, 181, 209 and 210) for a) dye deposited from methanol solution; b) dye-amylose mixture deposited from DMSO (non-inclusion complex); c) for dye-amylose mixture deposited from water (inclusion complex)

## Conclusion

For the amylose-dye inclusion complex, the interaction between helix cavity and dye is not strong enough to enhance the melting point transition. However, the dye in a constrained state does not degrade and escape from the cavity of amylose until the host has degraded.

* * *

The authors in the Naval Research Laboratory gratefully acknowledge the partial funding support from the Office of Naval Research.

## References

1 J. M. Lehn, Angew. Chem. Int. Ed. Engl., 29 (1990) 1304.
2 J. Szejtli, "Cyclodextrin Technology", Kluwer Academic Publishers, Netherlands 1988.
3 R. J. Bergeron in "Inclusion Compounds", Vol. 3 (ed. J. L. Atwood, J. E. D. Davies and D. D. MacNicol), Academic Press, New York 1984, pp. 391-443.
4 J. Szejtli, ibid., pp. 331-390.
5 W. Saenger, Angew. Chem., Int. Ed. Engl., 19 (1980) 344.
6 G. Wenz, ibid., 33 (1994) 803.
7 A. Harada, J. Li and M. Kamachi, Nature, 356 (1992) 325.
8 Y. Yamashita, J. Polym. Sci. part A, 3 (1965) 3251.
9 Y. Yamashita and N. Hirai, J. Polym. Sci., Polym. Phys. Ed., 4 (1966) 161.
10 Y. Yamashita and K. Monobe, J. Polym. Sci., Polym. Phys. Ed., 9 (1971) 1471.
11 H. Nakatani, K.-I. Shibata, H. Kondo and K. Hiromi, Biopolymers, 16 (1977) 2363.
12 T. Kuge and K. Takeo, Agr. Biol. Chem., 32 (1968) 1232.
13 G. Wulff and S. Kubik, Makromol. Chem., 193 (1992) 1071.
14 Y. Hui, X. Cheng, J. Gu and X. Jiang, Scientia Sinica (Series B), 25 (1982) 698.
15 Y. Hui, J. C. Russell and D. G. Whitten, J. Am. Chem. Soc., 105 (1983) 1374.
16 B. R. Suddaby, R. N. Dominey, Y. Hui and D. G. Whitten, Can. J. Chem. , 63 (1985) 1315.
17 M. T. AIIen, L. Miola, B. R. Suddaby and D. G. Whitten, Tetrahedron, 43 (1987) 1477.
18 O.-K. Kim and L. S. Choi, Langmuir, 10 (1994) 2842.
19 J. Szejtli and E. Bola, Starch, 32 (1980) 386.